

Assessment of Scalar Relativistic Effects on Halogen Bonding and σ -Hole Properties

Michal H. Kolář,^{*,†} Denisa Suchá,[‡] and Michal Pitoňák^{*,‡,¶}

[†]*Department of Physical Chemistry, University of Chemistry and Technology, Technická 5, 16628 Prague, Czech Republic*

[‡]*Department of Physical and Theoretical Chemistry, Faculty of Natural Sciences, Comenius University, Mlynská Dolina, 842 15 Bratislava, Slovakia*

[¶]*Computing Center of the Slovak Academy of Sciences, Dúbravská cesta č. 9, 845 35 Bratislava, Slovakia*

E-mail: michal@mhko.science; michal.pitonak@uniba.sk

Abstract

Halogen bond (X-bond) is a noncovalent interaction between a halogen atom and an electron donor. It is often rationalized by a region of the positive electrostatic potential on the halogen atom, so-called σ -hole. The X-bond strength increases with the atomic number of the halogen involved, thus for heavier halogens, relativistic effects become of concern. This poses a challenge for the quantum chemical description of X-bonded complexes. To quantify scalar relativistic effects (SREs) on the interaction energies and σ -hole properties, we have performed highly accurate coupled-cluster calculations at the complete basis set limit of several X-bonded complexes and their halogenated monomers. The SREs turned to be comparable in magnitude to the effect of basis set. The nonrelativistic calculations typically underestimate the attraction by up to 5% or 23% for brominated and iodinated complexes, respectively. Counter-intuitively, the electron densities at the bond critical points are larger for SRE-free calculations than for the relativistic ones. SREs yield smaller, flatter, and more positive σ -holes. Finally, we highlight the importance of diffuse functions in the basis sets and provide quantitative arguments for using basis sets with pseudopotentials as an affordable alternative to a more rigorous Douglas-Kroll-Hess relativistic theory.

1 Introduction

Halogen bonds (X-bonds) are attractive interactions involving a halogen and a nucleophile. For the last two decades, they have grown to a notable noncovalent interaction with great potential in many areas of chemistry.¹ They have been utilized in material design to organize molecules to the desired crystalline forms.² The supramolecular chemists benefit from the powerful ability of X-bonds to direct self-assembly in solution.^{3,4} Similarly, the specificity of the interaction helped design new catalysts⁵ or modulate the action of existing ones.^{6,7} In medicinal chemistry, the X-bonds are responsible for specific binding of halogenated ligands to biomolecules^{8,9} which is reflected by the growing number of X-bonded complexes recognized.

What makes the X-bond particularly appealing for modern chemistry is its high directionality¹⁰ and the possibility to ‘tune’ its strength. This is achieved either by exchanging the halogen atom involved in the interaction or by modifications in its chemical environment as suggested by theoretical work,^{11,12} although the practical use of the tuning is still not fully exploited.¹³

The rigorous definition of X-bond is rather recent,¹⁴ despite the evidence of the puzzling attraction between halogens and electron-rich species stretching back to the 19th century.¹⁵ There have been presented various views on X-bonds and their nature.^{16–18} Perhaps the most successful rationalization of X-bonding was proposed by Politzer and co-workers who identified a region of positive electrostatic potential (ESP) located in the elongation of the R–X covalent bond.¹⁹ Later on, the region was called σ -hole²⁰ and its concept was expanded to other groups of the periodic table.^{21,22}

Substantial work has been done on the theory of X-bonding.²³ Nevertheless, the accurate computational description of X-bonds is still challenging. The computations deal with all difficulties connected with an accurate description of noncovalent interactions in general.²⁴ Let us name the basis set superposition error (BSSE), necessity to use diffuse atomic orbital (AO) basis functions, or the quality correlation effects treatment, should the dispersion energy play an important role. Naturally, the higher accuracy is required, the more computationally intensive the calculations are.

In addition to the aforementioned aspects, proper computational treatment of chemical systems containing heavy elements needs to consider relativistic effects. These are known to affect practically all atomic or molecular properties, and their importance tends to grow with the atomic mass.²⁵

In the case of large (typically nonsymmetric) closed-shell systems, such as the ones studied in this work, relativity treatment can be reduced to so-called scalar (or spin-independent) relativistic effects (SREs),^{26,27} if errors up to few (typically, tenths of) percents in interaction energies are tolerable.²⁸ This is a substantial simplification as the neglect of spin-orbit (SO) coupling makes calculations of extended molecular complexes computationally feasible. The use of a relativistic one-component Hamiltonian (instead of four- or two-component) approach comes with practically negligible overhead compared to nonrelativistic one.

In practice, two major routes to SREs treatment are pursued. Either it is the all-electron approach utilizing one-component relativistic Hamiltonian, such as Douglas-Kroll-Hess (DKH) formalism^{29,30} (finite or infinite order), or the pseudopotential approach, in which the explicit core-electron interaction is replaced by a parametrized (often phenomenological) potential.³¹ Despite its simplicity, this less rigorous approximation was shown to perform surprisingly well for a wide range of atomic and molecular

properties and allows for even higher computational efficiency particularly at Hartree-Fock or Density Functional Theory level.

If we decompose a noncovalent interaction into electrostatic, induction, and dispersion forces, all of these contributions may be affected by SREs through dipole moments and dipole polarizabilities.²⁷ SREs for X-bonds may be important, because common halogens, bromine and iodine, possess high polarizabilities,³² so in some instances, X-bonding may be dispersion driven.³³ Holzer and Klopper studied³⁴ dispersion bound rare-gas dimers and small molecular complexes and argued that SREs should be considered for atoms beyond Kr.

Further in the context of noncovalent interactions, two studies reported contradictory results about relativistic effects in a gold-containing complex. While Anderson *et al.* observed new topological features of the electron density when the relativistic effects were considered,³⁵ Olejniczak *et al.* argued that these are not significant and confirmed “no relativityinduced noncovalent interactions” for the complex.³⁶

In the computational community, it was merely accepted that iodine SREs deserve special attention. Routinely, pseudopotentials are used in the chemical literature to treat SREs of iodine. Less frequently, higher-levels of relativistic theory (*e. g.* SO coupling) are applied such as in the recent work³⁷ focused on rare astatine X-bonded complexes.³⁸ The proper description of relativistic effects in astatine-containing molecules, as indicated also by other studies,^{28,39,40} is clearly more challenging compared to iodine and lighter halogens.

However, specific studies on the role of special relativity in X-bonding are rather sparse. Alkorta *et al.* studied the interactions of halogen diatomics with small Lewis bases⁴¹ using relativistic pseudopotentials and a two-component ZORA Hamiltonian.⁴² At the MP2 level with the triple- ζ basis set, they calculated various complex properties. While for the interaction energies the SREs were not assessed, a direct comparison of nonrelativistic and relativistic values was provided for NMR parameters. For instance, it was shown that the relativistic NMR chemical shifts are larger than their nonrelativistic counterparts.⁴¹

In this work, we perform quantum chemical calculations extrapolated to the complete basis set limit (CBS) using relativistic as well as nonrelativistic approaches. The use of a highly-accurate coupled cluster method allows us to dissect SREs from the effect of electron correlation treatment. Further the CBS extrapolation makes our conclusions independent of basis set size. Therefore we differentiate between the SREs and other effects in a comprehensive way.

We assess the impact of SREs on brominated and iodinated molecules and avoid any astatine, where non-scalar relativistic effects may play a role,²⁸ thus would go beyond our objectives. This is however only a minor limitation since the vast majority of studies focus on halogens up to iodine. Here, we calculate interaction energies of the X-bonded complexes, and on their electron density and ESP features. Understanding the role of SREs in the σ -hole properties should bring a transferable knowledge useful for applications regardless of the interacting partner of the halogen-containing molecules.

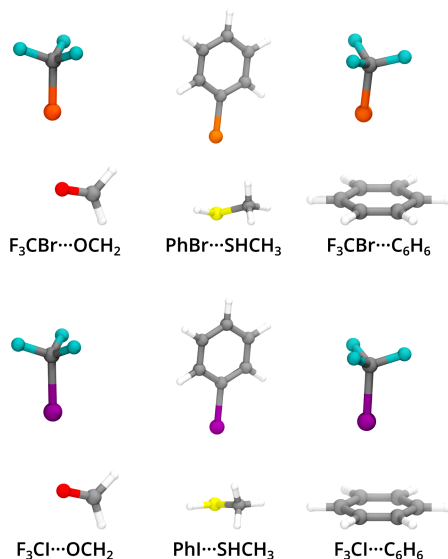


Figure 1: Geometries of the X-bonded complexes investigated. C gray, H white, F cyan, Br orange, I purple, S yellow.

2 Methods

2.1 Investigated Noncovalent Complexes and Basis Sets

The noncovalent complexes studied in this work were taken from the X40 data set of Řezáč *et al.*⁴³ The X40 data set contains benchmark interaction energies of noncovalent complexes, where halogen atoms participate in a variety of interaction motifs. In the original work, the X40 geometries of the complexes were optimized at the counterpoise-corrected⁴⁴ MP2/cc-pVTZ level, using pseudopotentials on halogen atoms. These geometries were used for our calculations without any further re-optimization. Here to probe diverse types of X-bonds, we selected a sample of six complexes from the X40, both aliphatic and aromatic (Figure 1). Four of them form an X-bond with a lone electron pair:

- trifluorobromomethane...formaldehyde ($\text{F}_3\text{CBr}\cdots\text{OCH}_2$)
- trifluoriodomethane...formaldehyde ($\text{F}_3\text{CI}\cdots\text{OCH}_2$)
- bromobenzene...methanethiol ($\text{PhBr}\cdots\text{SHCH}_3$)
- iodobenzene...methanethiol ($\text{PhI}\cdots\text{SHCH}_3$)

In the other two complexes, the X-bond directs towards a system of conjugated π -electrons:

- trifluorobromomethane...benzene ($\text{F}_3\text{CBr}\cdots\text{C}_6\text{H}_6$)
- trifluoriodomethane...benzene ($\text{F}_3\text{CI}\cdots\text{C}_6\text{H}_6$)

The selection of basis sets^{45,46} suitable for this study was not straightforward. Ideally, we would have tested a series of nonrelativistic basis sets (with increasing cardinal number ζ) and a complementary series, suitable for the side-by-side assessment of relativistic effects (using relativistic Hamiltonian and/or pseudopotential). The desire for

a *series* of basis sets is motivated by our intent to carry out basis set extrapolation of interaction energies towards the CBS limit, as they are known to converge rather slowly with the basis set size. Alternatively, we could choose explicitly correlated methods, but the availability of suitable (non)relativistic basis sets is even more limited.

The choice of basis sets for the bromine atom is somewhat wider than for iodine. For both halogen types, nonrelativistic XZP^{47–49} (X=D, T, or Q, for double- ζ , triple- ζ , and quadruple- ζ , respectively) and AXZP,^{50–52} as well as relativistic contractions for DKH Hamiltonian, XZP-DKH,⁵³ are available. Nonrelativistic correlation-consistent basis sets (aug-)cc-pVXZ⁵⁴ and DKH-optimized relativistic basis sets (aug-)cc-pVXZ-DK⁵⁵ are available for bromine only, but relativistic pseudopotentials (aug-)cc-pVXZ-PP⁵⁶ exist for both halogens. Another universal alternative for relativistic calculations is the ANO-RCC⁵⁷ basis set. Nonrelativistic ANO contractions were published as well, but not for heavier halogens than chlorine, so they were not used in this study.

2.2 Interaction Energies

Energies of complexes and their interacting subsystems were calculated using the coupled clusters method with iterative single- and double-excitations, corrected by perturbative inclusion of triple-excitations (CCSD(T)), wherever it was computationally feasible. The calculations in AQZP and aug-cc-pVQZ basis set of all complexes except for the smallest one – F₃CBr \cdots OCH₂, could only be carried out at the second-order Møller-Plesset perturbation theory level (MP2), and the well-established focal-point scheme⁵⁸ was applied to obtain an estimate of the $E_Q(\text{CCSD(T)})$ energies.

$$E_X(\text{CCSD(T)}) = E_X(\text{MP2}) + \Delta E_{X-1}(\text{CCSD(T)}) \quad (1)$$

where $\Delta E_{X-1}(\text{CCSD(T)})$ is the difference of CCSD(T) and MP2 energies in basis set with lower cardinality “X – 1”.

Energies at the CBS limit were estimated according to Halkier *et al.*⁵⁹ using the extrapolation formula

$$\Delta E_X = \Delta E_{CBS} + k \cdot X^{-3} \quad (2)$$

from triple- and quadruple- ζ basis sets, where X is 3 for triple- and 4 for quadruple- ζ basis, and k is a fitting constant. Interaction energies were corrected for BSSE using the counterpoise method.⁴⁴

All calculations were carried out using NWChem 6.6 program package.⁶⁰ The default threshold (of 10⁻⁵ a.u.) for the elimination of linearly dependent AO basis functions had to be increased to achieve convergence of orbital optimization in some cases (Table S1). The third-order DKH approximation with cross-product integral terms⁶¹ was used in all-electron relativistic calculations.

2.3 Bond Critical Points

For all complexes, the electron densities were exported from the NWChem as cube files and analyzed by the Topology Toolkit extension⁶² of the Paraview program package.⁶³ The electron densities were reported for the bond critical points (BCPs), *i. e.* the (3, –1) critical points of the electron density.⁶⁴ The analysis was carried out for all basis sets and relativity treatments investigated with the additional aim to correlate the BCPs density ρ_{BCP} values with the interaction energies.

2.4 Monomer Properties

To characterize the halogen σ -holes, electron densities and ESPs were analyzed at various *ab initio* levels. The supermolecular geometries of the monomers F_3CBr , F_3CI , $PheBr$, and $PheI$, as taken from the X40 data set, were used without further energy optimization. The analyses rested on the molecular surface defined as the isosurface of electron density of 0.001 e/bohr^3 ,⁶⁵ which is a common threshold used in the context of X-bonding.²³

The principal halogen covalently bound to a molecule is not a perfect sphere,⁶⁶ thus its size cannot be described by a single radius. Here, we use two radii to characterize the halogen size: i) the parallel radius r_{\parallel} is a distance from the halogen to the electron density isosurface in the direction of C–X bond, ii) the perpendicular radius r_{\perp} is equivalent distance, but in the direction perpendicular to the C–X bond. While the r_{\perp} is uniquely defined for molecules with C_{∞} symmetry (*e.g.* dihalogens), it must be explicitly specified in all other cases. Here for halogenbenzenes, we calculated r_{\perp} as the arithmetic mean of two values: one r_{\perp} lying in the aromatic plane, and the other perpendicular to it and to C–X bond at the same time. In the case of halomethanes, r_{\perp} was calculated as the average of r_{\perp} in the plane defined by X, carbon and one fluorine atom, and r_{\perp} in the direction perpendicular to this plane.

The difference of the two radii represents the absolute value of polar flattening v_{pf} , as discussed in detail in ref. 66. Here, we focus on the ratio of v_{pf} and r_{\perp} expressed in percents and denominated as the relative polar flattening $rv_{pf} = 100 \cdot (1 - \frac{r_{\parallel}}{r_{\perp}})$. The rv_{pf} describes how the halogen shape deviates from an ideal sphere.

The σ -hole magnitude V_{\max} was calculated as the maximum of the ESP on the molecular surface in the extension of the C–X bond, as detailed in ref. 10. All monomer calculations were based on the results of DPLOT and ESP modules of the NWChem package.⁶⁰ Most of the analyses used NumPy⁶⁷ and Matplotlib⁶⁸ Python libraries.

3 Results and Discussion

3.1 Characteristics of the Halogenated Monomers

We describe how monomer characteristics vary with the SRE treatment, basis set type, and size. Because a wider range of basis sets is available for bromine than for iodine, we discuss the brominated monomers first, and later move to the iodinated ones.

Figure 2 shows the r_{\parallel} , rv_{pf} , and V_{\max} calculated for various basis sets and SRE treatment for the F_3CBr and $PhBr$. We assess the SREs on the monomer characteristics using values calculated in the largest available basis set, *i.e.* the quadruple- ζ (QZ). The qualitative conclusions that bromine on the F_3CBr is smaller and more positive than the bromine on $PhBr$ are true regardless of the inclusion or exclusion of SREs. Quantitatively on both monomers, the bromine appears smaller, flatter, and more positive when the SREs are taken into account (Figure 2). The differences between relativistic and nonrelativistic values are very small, however: about 0.01 \AA for r_{\parallel} , 0.2 per cent point for rv_{pf} and 0.001 a.u. for V_{\max} .

For the aug-cc-pVXZ and cc-pVXZ basis sets, a comparison of two relativistic approaches – DKH and pseudopotentials – is possible. In all monomer characteristics studied, the values are practically identical in the QZ basis set. Hence, it is beneficial to use the pseudopotential approach due to its lower computational demands compared

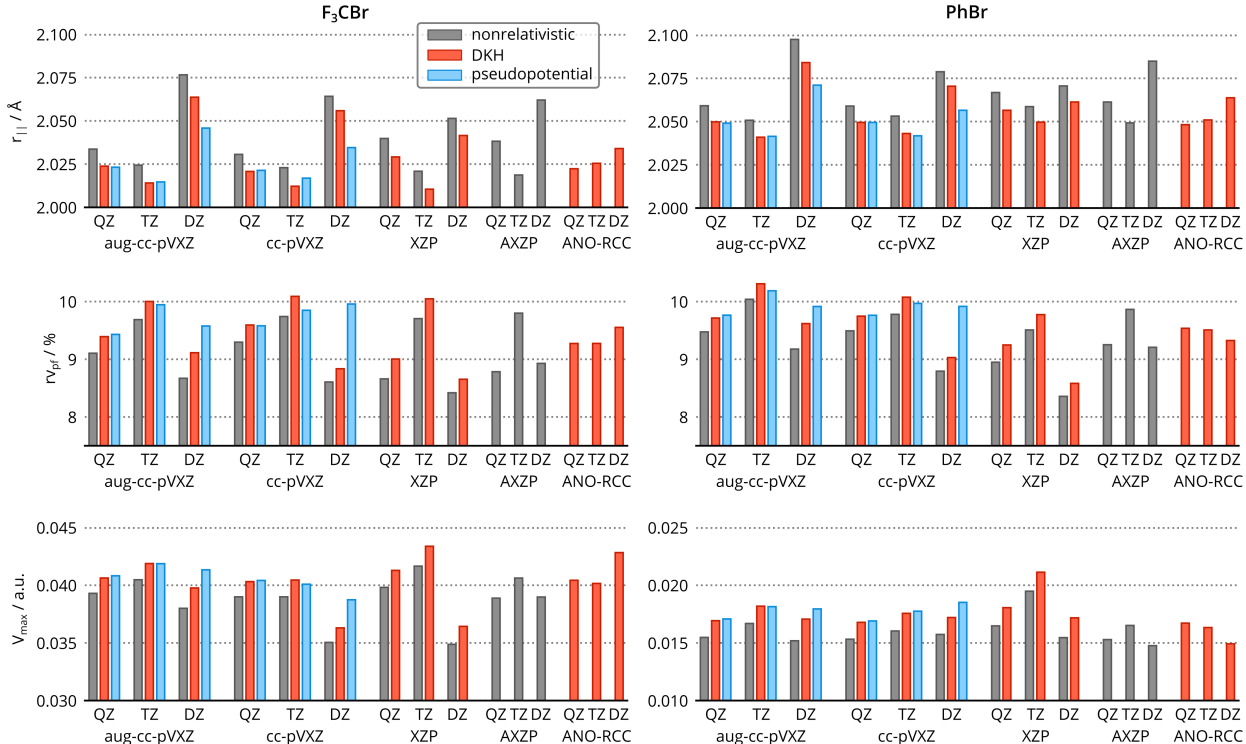


Figure 2: The parallel halogen radius r_{\parallel} , relative polar flattening rv_{pf} and σ -hole magnitude V_{max} of F_3CBr (left) and PhBr (right) calculated using various basis sets. Nonrelativistic (gray) and relativistic calculations using DKH (red) and pseudopotential (blue) approaches are compared, whenever possible.

to DKH, at least in one-electron approximations. A larger difference between DKH and pseudopotential treatment is observed for a double- ζ (DZ) basis set, especially for rv_{pf} at the cc-pVDZ level. However, if we compare the DZ values with the reference QZ values with DKH treatment, the DZ with pseudopotential performs better than DZ-DKH, most likely due to a favorable compensation of errors.

The effect of basis-set size and basis-set type, which was reported previously for other basis sets and molecules,^{23,69} is often larger than the SREs. Overall, it has a little effect on qualitative conclusions about bromine’s r_{\parallel} , rv_{pf} and V_{max} on the two monomers. Interestingly, low variations of σ -hole magnitude were obtained for the PhBr , which means that V_{max} of this system is less sensitive to basis set quality than F_3CBr .

For iodine, the nonrelativistic basis sets are less reasonable than for bromine due to iodine’s higher mass. That is perhaps the reason why a narrower range of nonrelativistic basis sets is available. The r_{\parallel} , rv_{pf} and V_{max} for the iodinated monomers F_3CI and PhI are in Figure 3. A direct comparison between nonrelativistic and relativistic values is only possible for the XZP series. Alike bromine, taking SREs into account for iodine results in a smaller, flatter, and more positive atom compared to the nonrelativistic calculations. These qualitative conclusions are independent on basis set size. On the other hand, the values of the monomer characteristics often depend on the basis-set size more than on the relativity treatment. For instance, for F_3CI , the V_{max} difference

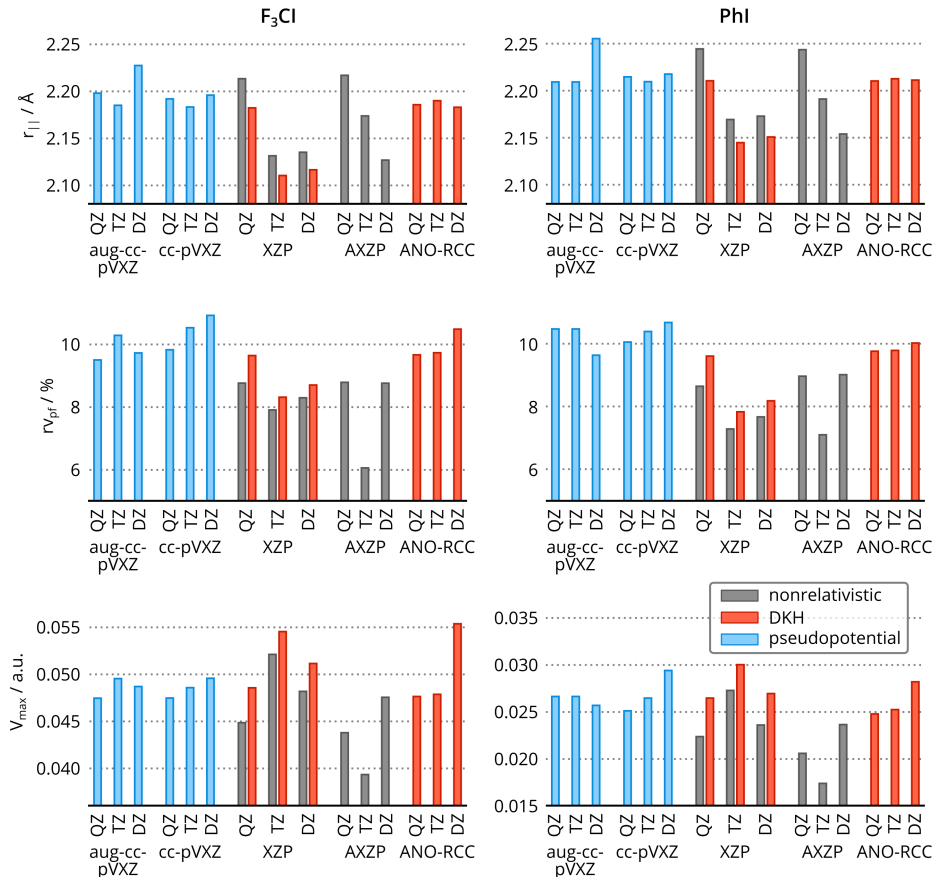


Figure 3: The parallel radius $r_{||}$, relative polar flattening rv_{pf} and σ -hole magnitude V_{max} of F_3CI (left) and ΦI (right) calculated using various basis sets. Nonrelativistic (gray) and relativistic calculations using DKH (red) and pseudopotential (blue) approaches are compared, whenever possible.

between QZP and TZP is about twice as large as the difference between QZP and QZP-DKH (Figure 3).

Following the chemical intuition, the extent of SREs is larger for iodine than for bromine for all three monomer characteristics. The differences between values with and without SREs are roughly 0.03 \AA of $r_{||}$, about 1 per cent point of rv_{pf} , and 0.004 a.u. of V_{max} (comparing QZP values).

Further, we investigate how much the iodine characteristics differ from the bromine characteristics and how these differences vary with the basis set and SREs. In other words, we want to know how SREs affect the relative comparison of the two halogens. Figure 4 shows the ratios $A(I)/A(Br) \cdot 100$, where A stands for $r_{||}$, rv_{pf} , or V_{max} . Note that we compare only those *ab initio* levels, which are available for iodine.

All calculations predict that iodine is larger than bromine (in a sense of $r_{||}$) no matter what basis set or relativity treatment is used. The Dunning’s (aug-)cc-pVXZ are remarkably consistent yielding iodine larger by 8% than bromine. The same results are obtained for all ANO-RCC and QZ basis sets in general. There is a stronger dependence of $r_{||}$ on the basis set size for XZP and AXZP series.

A notable qualitative effect of scalar relativity is observed for the iodine/bromine

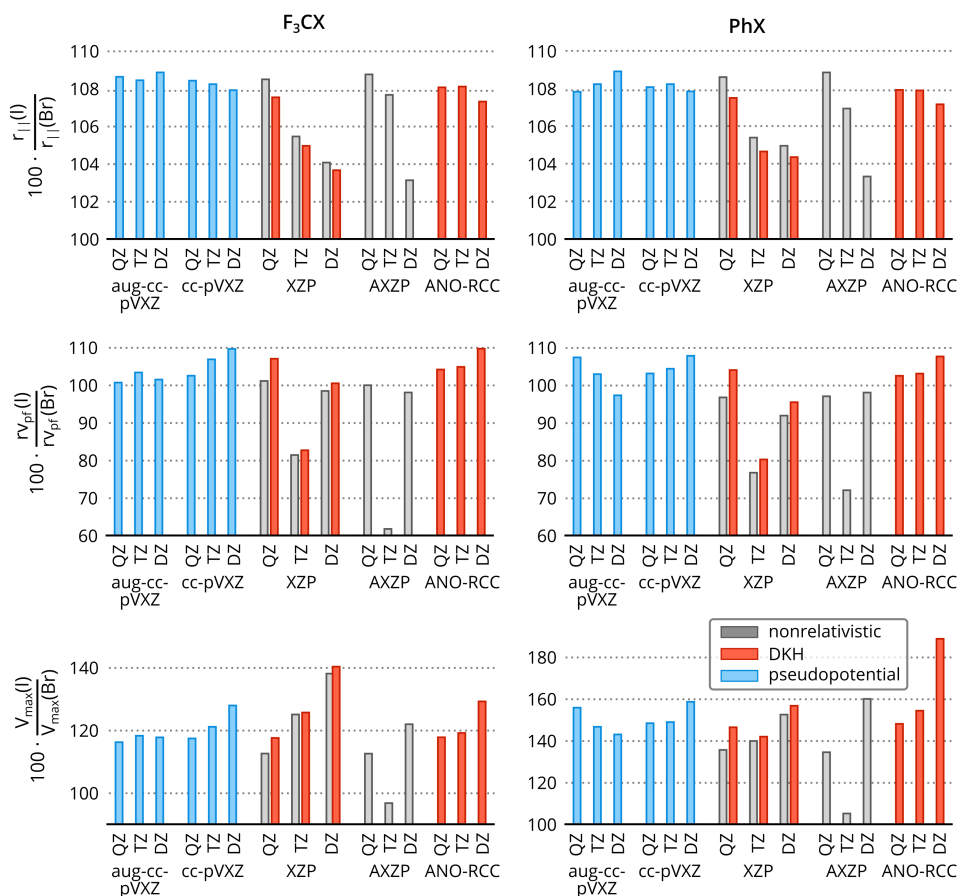


Figure 4: Ratios of the parallel radius $r_{||}$, relative polar flattening rv_{pf} and σ -hole magnitude V_{max} of iodinated and brominated monomers. Nonrelativistic (gray) and relativistic calculations using DKH (red) and pseudopotential (blue) approaches are compared, when possible.

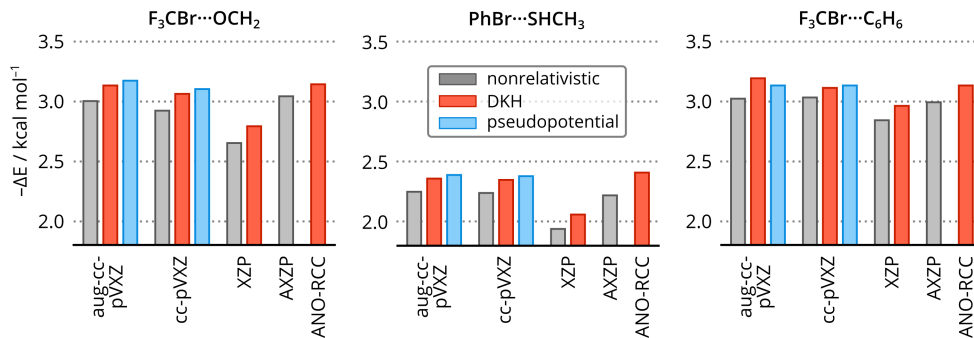


Figure 5: The effect of basis-set type and size and of relativity treatment on interaction energies (ΔE) of noncovalent complexes containing bromine. CP-corrected interaction energies extrapolated towards the CBS limit with nonrelativistic (gray), DKH-Hamiltonian optimized (red) and pseudopotential (blue) basis sets using frozen-core approximation are compared, whenever possible.

ratio of rv_{pf} . While the relativistic calculations conclude that iodine is flatter than bromine on both trifluoromethyl as well as phenyl moieties ($rv_{pf}(\text{I})/rv_{pf}(\text{Br}) > 1$), the nonrelativistic calculations predict the opposite. The effect of basis set is even larger: TZP and ATZP incorrectly predict iodine being less flattened than bromine by more than 25%. More realistic results of DZP and ADZP are likely caused by the favorable compensation of errors.

The σ -hole magnitude is consistently predicted larger (more positive) for iodine compared to bromine, which goes in line with the notion in the X-bonding research community. The exception is the nonrelativistic ATZP, which puts the two halogens roughly on par and performs worse than the equivalent basis set of double- ζ size.

An important finding is that the pseudopotential calculations yield iodine/bromine ratios of monomer characteristics similar to the DKH values of both XZP and ANO-RCC series. This provides strong support for using pseudopotential calculations as a less demanding alternative to DKH treatment of SREs on halogenated molecules.

3.2 Interaction energies

Interaction energy should reflect the properties of interacting monomers, particularly if electrostatic energy is non-negligible, which is the case of the X-bond. Because the V_{\max} values are larger when a relativistic approach is used, we would expect stronger intermolecular interaction for the relativistic calculations than for the nonrelativistic ones. On the other hand, X-bond is a superposition of many interaction energy components including *e.g.* notable dispersion contribution and often it is not the exclusive interaction between the subsystems. The overall impact of SREs inclusion may thus be slightly smeared on the level of total interaction energies.

We inspect the brominated complexes, whose interaction energies obtained for several series of basis sets and SRE treatments are summarized in Figure 5. In general, the intermolecular interactions are slightly stronger when calculated at relativistic level, *i.e.* the relativistic interaction energies are more negative than the nonrelativistic ones. The more positive relativistic σ -holes agree with this finding. For brominated com-

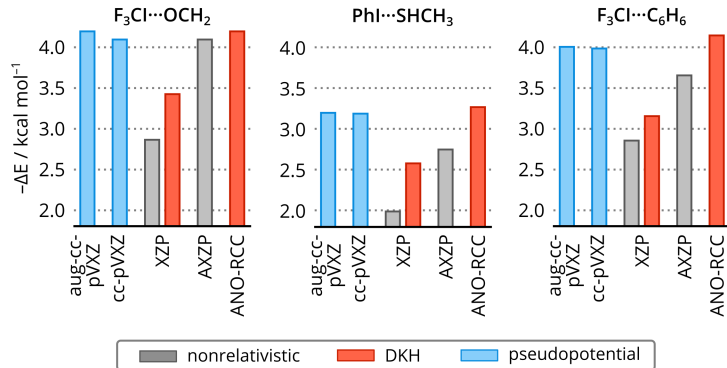


Figure 6: The effect of basis set quality and relativity treatment on interaction energies (ΔE) of noncovalent complexes containing iodine. CP-corrected interaction energies extrapolated towards the CBS limit with nonrelativistic (gray), DKH-Hamiltonian optimized (red) and pseudopotential (blue) basis sets using frozen-core approximation are compared, whenever possible.

plexes, the SREs are in the order of about 5% (or 0.1 kcal/mol). A comparison within (aug-)cc-pVXZ reveals that ΔE at pseudopotential level is a bit higher than at DKH level, but still, the (relativistic) pseudopotential approach is closer to the reference (relativistic) DKH value than the nonrelativistic calculation.

The basis set has a stronger impact on ΔE than the SREs. The XZP basis sets show the largest deviation from the rest of the results, regardless of the SREs inclusion, while AXZP and aug-cc-pVXZ basis sets deliver similar results. The XZP-DKH is by about 0.2–0.4 kcal/mol less negative than ANO-RCC (or aug-cc-pVXZ-DKH), which is about twice as much as the difference from nonrelativistic XZP values. Note that the basis-set size dependence of ΔE is damped by extrapolation towards CBS, so the variations are attributable to the basis set quality, *i. e.* mostly sufficient presence of diffuse basis functions.

For the iodinated complexes, the interaction energy plots are shown in Figure 6. Only the XZP basis set allows assessing the SREs directly. For all three complexes, the relativistic ΔE with XZP is always more negative than the nonrelativistic. Like in the bromine case, the interaction between the monomers is stronger when the SREs are taken into account. However, in complexes with iodine, the SREs are more pronounced and increase to almost 23% (0.59 kcal/mol for PhI···SHCH₃).

Further, a more refined analysis is possible through ΔE values summarized in Tables S2 and S3. In the case of the smallest investigated system, F₃CBr···OCH₂, we provide a full comparison of the extrapolated interaction energies obtained using the focal-point scheme (Eq. 1) and the ‘plain scheme’, where CCSD(T) energies are calculated in quadruple- ζ basis sets. Deviations for the largest basis sets (AXZP and aug-cc-pVXZ(-DKH/-PP)), for which the focal-point scheme is used to obtain benchmark ΔE s for larger complexes, are in the order of hundredths of kcal/mol. The deviations are more pronounced in smaller basis sets (up to about 0.1 kcal/mol or 4%), which is understandable, if we take into account insufficient basis set saturation of the ΔE_{X-1} (CCSD(T)) term.

The extrapolated ΔE s for the bromine-containing species (Table S2) calculated in aug-cc-pVXZ-DKH basis set with SREs inclusion using DKH Hamiltonian are consid-

ered as the benchmark in this work. Should we accept the monotonous character of the ΔE convergence with the basis set size (or cardinality), aug-cc-pVXZ-type basis sets exhibit slightly better saturation compared to ANO-RCC and AXZP basis sets. In the case of ANO-RCC basis sets this can be reasoned by a notably lower number of basis functions (by almost 40%; 420, 726 and 724 for ANO-RCC quadruple- ζ contraction *vs.* 665, 1151 and 1169 for aug-cc-pVQZ for $F_3CBr \cdots OCH_2$, $PheBr \cdots SHCH_3$, and $F_3CBr \cdots C_6H_6$, respectively), unlike in the case of AXZP basis sets, which have even slightly more basis functions (by about 4 – 7%) than aug-cc-pVXZ basis sets. Concerning the ways of SREs inclusion, the use of pseudopotential appears to be as good choice as the use of DKH Hamiltonian, as their mutual difference in interaction energies ranges between 0.03 – 0.06 kcal/mol.

Detailed analysis of the ΔE s for iodine-containing species (Table S3) is rather restricted, due to the aforementioned limited availability of systematically optimized basis set series for iodine. In this case, the most accurate ΔE s with SREs inclusion using DKH Hamiltonian are obtained in ANO-RCC basis sets, which are notably less saturated compared to aug-cc-pVXZ basis sets with pseudopotentials. The differences between these two sets of results are, however, quite small ranging from zero for $F_3CI \cdots OCH_2$ to 0.14 kcal/mol for $F_3CI \cdots C_6H_6$. This comparison is even more problematic due to the fact, that ANO-RCC results are obtained using full CCSD(T) calculations, while the results in aug-cc-pVXZ-PP series are obtained using focal-point scheme potentially introducing additional uncertainty. Nevertheless, the deviation from the most accurate nonrelativistic results (obtained using AXZP basis sets) can still be identified, particularly in the case of $PheI \cdots SHCH_3$, where it reaches the maximum of 0.45 kcal/mol (about 16%, decreases from 0.73 at double- ζ to 0.51 kcal/mol at quadruple- ζ level).

3.3 Bond Critical Points

The values of electron density at BPCs are shown in Figure 7. They span a range between 0.006 and 0.017 a.u. ρ_{BCP} is slightly sensitive to the basis set quality and size as well as to the treatment of SREs. The largest variations are observed for $F_3CI \cdots OCH_2$ complex. In all cases, where it was possible to compare, the relativistic ρ_{BCP} is smaller than the nonrelativistic. The difference is about 1% for complexes containing bromine, and about 4% for complexes containing iodine.

Previously, it was shown that ρ_{BCP} is a measure of interaction strength of noncovalent complexes,^{70–72} so we analyzed the 432 pairs of ρ_{BCP} and ΔE collected here. Figure 8 shows the regression plots for the quadruple- ζ basis sets common for brominated and iodinated complexes. Bearing in mind the small number of complexes, we observe only a poor correlation. Here the complexes are more diverse and span a smaller range of interaction energies than in previous studies, where systematic sets of complexes shown higher correlations.^{73,74} Overall, a wider set to complexes would be needed to draw any conclusions about the role of SREs on the correlation between ρ_{BCP} and ΔE .

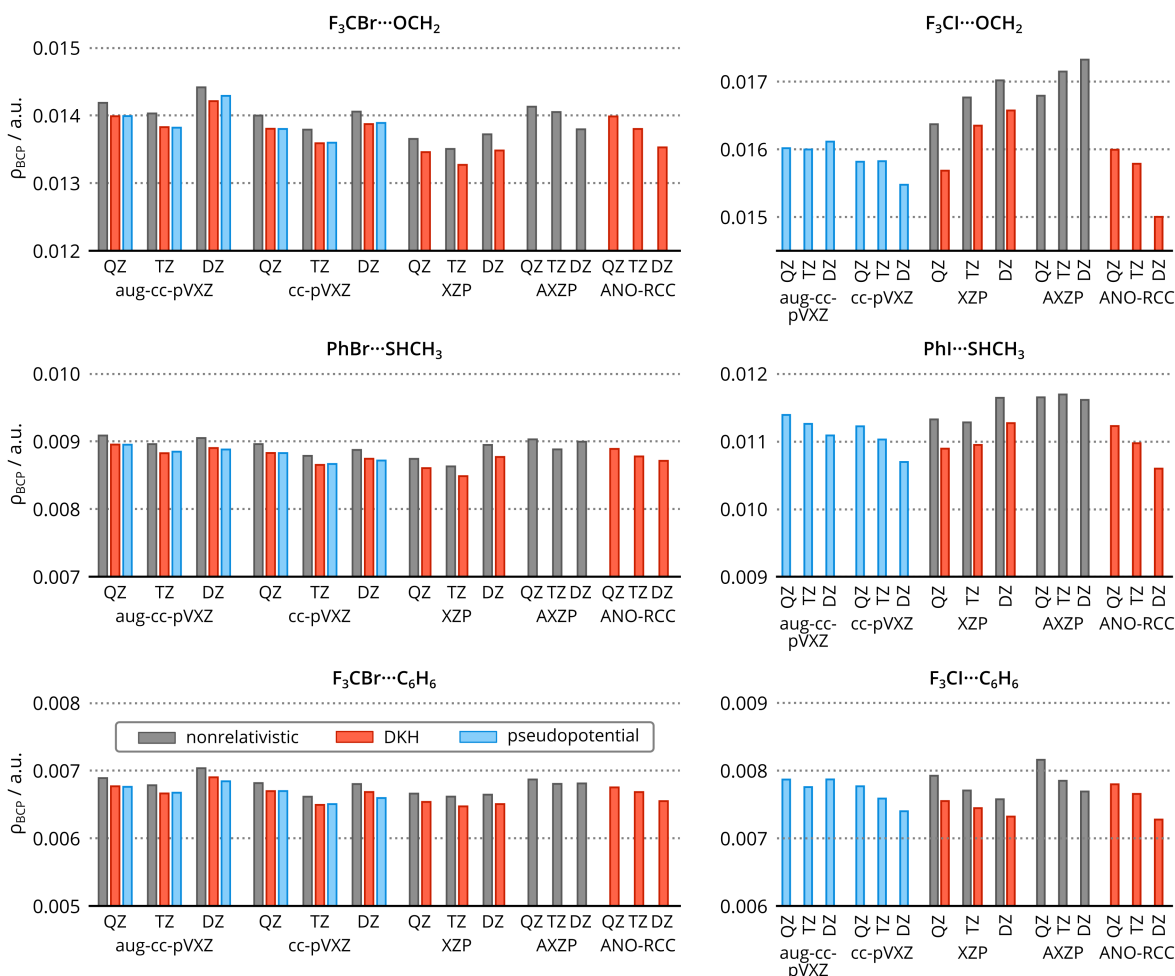


Figure 7: Electron densities ρ_{BCP} at the bond critical points with nonrelativistic (gray), DKH-Hamiltonian optimized (red) and pseudopotential (blue) basis sets using frozen-core approximation. Note the common Y-axis extent for all of the complexes ($3 \cdot 10^{-3}$ a.u.).

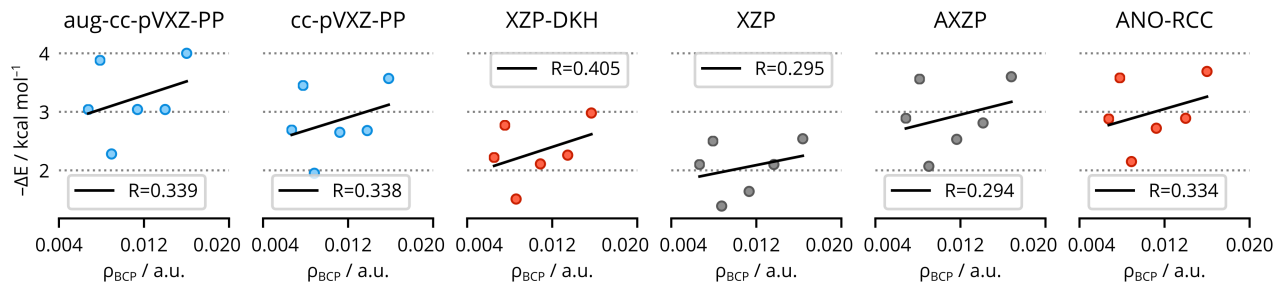


Figure 8: A correlation between the electron density at the bond critical points (ρ_{BCP} and the interaction energy (ΔE). The scatter points are color coded according to the SRE treatment, *e.g.* nonrelativistic in gray, relativistic pseudopotential in blue, and relativistic DKH in red.

4 Conclusions

In this work, we provide a detailed analysis of the impact of scalar relativistic effects on properties of σ -hole and of X-bonds. Using CCSD(T)/CSB – the golden standard of noncovalent calculations – we eliminate inaccuracies related to the electron correlation. By carrying out calculations in a series of systematically optimized basis sets we detach the effect of basis set incompleteness from SREs, which turned out to be a challenging task, in particular for iodine-containing species.

In general, the SREs are small for all investigated quantities of halogenated monomers and X-bonded complexes. The magnitude of SREs is intuitively larger for iodine than for bromine. For brominated complexes, the SREs are mostly negligible (<5%). SRE treatment is essential for iodinated molecules/complexes, where the error brought by the neglect of SREs may reach several tens of percent.

We found that the magnitude of basis set effects on interaction energies and σ -hole properties is on par to or even larger than SREs. The proper choice of basis set is thus as critical as the ways of SRE treatment. Smaller double- ζ basis sets sometimes performed better than triple- ζ basis sets perhaps due to error compensation, which increases the motivation to use extrapolation to CBS.

Calculations with relativistic pseudopotentials delivered results similar to those from all-electron calculations using relativistic Hamiltonian.

Funding Information

This work was supported by the Slovak Research and Development Agency, contract No. APVV-15-0105, and Slovak Grant Agency VEGA under the contract no. 1/0777/19.

Research Resources

Part of the calculations was performed in the Computing Center of the Slovak Academy of Sciences using the supercomputing infrastructure acquired in project ITMS 26230120002 and 26210120002 (Slovak infrastructure for high-performance computing) supported by the Research & Development Operational Programme funded by the ERDF.

Author Contributions

MP designed the research. DS and MP performed quantum chemical calculations. MHK evaluated monomer properties. All of the authors evaluated properties of noncovalent complexes and drafted the manuscript. MHK and MP finalized the manuscript.

Supplementary Information

The number of eliminated basis set functions due to linear dependence, and the interaction energies of all complexes at all levels of theory are provided in Tables S1, S2 and S3.

References

- (1) Cavallo, G.; Metrangolo, P.; Milani, R.; Pilati, T.; Priimagi, A.; Resnati, G.; Terraneo, G. The halogen bond. *Chem. Rev.* **2016**, *116*, 2478–2601.
- (2) Metrangolo, P.; Meyer, F.; Pilati, T.; Resnati, G.; Terraneo, G. Halogen bonding in supramolecular chemistry. *Angew. Chem. Int. Ed. Engl.* **2008**, *47*, 6114–6127.
- (3) Gilday, L. C.; Robinson, S. W.; Barendt, T. A.; Langton, M. J.; Mullaney, B. R.; Beer, P. D. Halogen bonding in supramolecular chemistry. *Chem. Rev.* **2015**, *115*, 7118–7195.
- (4) Brown, A.; Beer, P. D. Halogen bonding anion recognition. *Chem. Commun.* **2016**, *52*, 8645–8658.
- (5) Carreras, L.; Serrano-Torné, M.; van Leeuwen, P. W.; Vidal-Ferran, A. XBphos-Rh: a halogen-bond assembled supramolecular catalyst. *Chem. Sci.* **2018**, *9*, 3644–3648.
- (6) Bulfield, D.; Huber, S. M. Halogen bonding in organic synthesis and organocatalysis. *Chem. Eur. J.* **2016**, *22*, 14434–14450.
- (7) Carreras, L.; Benet-Buchholz, J.; Franconetti, A.; Frontera, A.; van Leeuwen, P. W.; Vidal-Ferran, A. Halogen bonding effects on the outcome of reactions at metal centres. *Chem. Commun.* **2019**, *55*, 2380–2383.
- (8) Wilcken, R.; Zimmermann, M. O.; Lange, A.; Joerger, A. C.; Boeckler, F. M. Principles and applications of halogen bonding in medicinal chemistry and chemical biology. *J. Med. Chem.* **2013**, *56*, 1363–1388.
- (9) Mendez, L.; Henriquez, G.; Sirimulla, S.; Narayan, M. Looking back, looking forward at halogen bonding in drug discovery. *Molecules* **2017**, *22*, 1397.
- (10) Kolář, M.; Hostaš, J.; Hobza, P. The strength and directionality of a halogen bond are co-determined by the magnitude and size of the σ -hole. *Phys. Chem. Chem. Phys.* **2014**, *16*, 9987–9996.
- (11) Riley, K. E.; Murray, J. S.; Fanfrlík, J.; Řezáč, J.; Solá, R. J.; Concha, M. C.; Ramos, F. M.; Politzer, P. Halogen bond tunability I: the effects of aromatic fluorine substitution on the strengths of halogen-bonding interactions involving chlorine, bromine, and iodine. *J. Mol. Model.* **2011**, *17*, 3309–3318.
- (12) Riley, K. E.; Murray, J. S.; Fanfrlík, J.; Řezáč, J.; Solá, R. J.; Concha, M. C.; Ramos, F. M.; Politzer, P. Halogen bond tunability II: the varying roles of electrostatic and dispersion contributions to attraction in halogen bonds. *J. Mol. Model.* **2013**, *19*, 4651–4659.
- (13) Fanfrlík, J.; Kolář, M.; Kamlar, M.; Hurný, D.; Ruiz, F. X.; Cousido-Siah, A.; Mitschler, A.; Řezáč, J.; Munusamy, E.; Lepšík, M.; Matějčík, P.; Veselý, J.; Podjarný, A.; Hobza, P. Modulation of aldose reductase inhibition by halogen bond tuning. *ACS Chem. Biol.* **2013**, *8*, 2484–2492.

- (14) Desiraju, G. R.; Ho, P. S.; Kloo, L.; Legon, A. C.; Marquardt, R.; Metrangolo, P.; Politzer, P.; Resnati, G.; Rissanen, K. Definition of the halogen bond (IUPAC recommendations 2013). *Pure Appl. Chem.* **2013**, *85*, 1711–1713.
- (15) Guthrie, F. XXVIII. On the iodide of iodammonium. *J. Chem. Soc.* **1863**, *16*, 239–244.
- (16) Eskandari, K.; Zariny, H. Halogen bonding: A lump–hole interaction. *Chem. Phys. Lett.* **2010**, *492*, 9–13.
- (17) Palusiak, M. On the nature of halogen bond–The Kohn–Sham molecular orbital approach. *J. Mol. Struct. THEOCHEM* **2010**, *945*, 89–92.
- (18) Wang, C.; Danovich, D.; Mo, Y.; Shaik, S. On the nature of the halogen bond. *J. Chem. Theory Comput.* **2014**, *10*, 3726–3737.
- (19) Brinck, T.; Murray, J. S.; Politzer, P. Surface electrostatic potentials of halogenated methanes as indicators of directional intermolecular interactions. *Int. J. Quantum Chem.* **1992**, *44*, 57–64.
- (20) Clark, T.; Hennemann, M.; Murray, J. S.; Politzer, P. Halogen bonding: the σ -hole. *J. Mol. Model.* **2007**, *13*, 291–296.
- (21) Murray, J. S.; Lane, P.; Politzer, P. Expansion of the σ -hole concept. *J. Mol. Model.* **2009**, *15*, 723–729.
- (22) Murray, J. S.; Riley, K. E.; Politzer, P.; Clark, T. Directional weak intermolecular interactions: σ -hole bonding. *Aust. J. Chem.* **2010**, *63*, 1598–1607.
- (23) Kolář, M. H.; Hobza, P. Computer modeling of halogen bonds and other σ -hole interactions. *Chem. Rev.* **2016**, *116*, 5155–5187.
- (24) Řezáč, J.; Hobza, P. Benchmark Calculations of Interaction Energies in Noncovalent Complexes and Their Applications. *Chem. Rev.* **2016**, *116*, 5038–5071.
- (25) Pyykkö, P. Relativistic effects in chemistry: more common than you thought. *Ann. Rev. Phys. Chem.* **2012**, *63*, 45–64.
- (26) Almlf, J.; Gropen, O. *Reviews in Computational Chemistry*; John Wiley & Sons, Ltd, 2007; pp 203–244.
- (27) Ilias, M.; Kelloe, V.; Urban, M. Relativistic effects in atomic and molecular properties. *Acta Phys. Slovaca* **2010**, *60*, 259–391.
- (28) Galland, N.; Montavon, G.; Le Questel, J.-Y.; Graton, J. Quantum calculations of At-mediated halogen bonds: on the influence of relativistic effects. *New J. Chem.* **2018**, *42*, 10510–10517.
- (29) Nakajima, T.; Hirao, K. The Douglas-Kroll-Hess approach. *Chem. Rev.* **2012**, *112*, 385–402.
- (30) Reiher, M. Relativistic Douglas-Kroll-Hess theory. *WIREs Comput. Mol. Sci.* **2012**, *2*, 139–149.

- (31) Schwerdtfeger, P. The pseudopotential approximation in electronic structure theory. *ChemPhysChem* **2011**, *12*, 3143–3155.
- (32) de Jong, W.; Styszynski, J.; Visscher, L.; Nieuwpoort, W. Relativistic and correlation effects on molecular properties: The interhalogens ClF, BrF, BrCl, IF, ICl, and IBr. *J. Chem. Phys.* **1998**, *108*, 5177–5184.
- (33) Riley, K. E.; Hobza, P. The relative roles of electrostatics and dispersion in the stabilization of halogen bonds. *Phys. Chem. Chem. Phys.* **2013**, *15*, 17742–17751.
- (34) Holzer, C.; Klopper, W. Quasi-relativistic two-component computations of intermolecular dispersion energies. *Mol. Phys.* **2017**, *115*, 2775–2781.
- (35) Anderson, J. S.; Rodríguez, J. I.; Ayers, P. W.; Trujillo-González, D. E.; Götz, A. W.; Autschbach, J.; Castillo-Alvarado, F. L.; Yamashita, K. Molecular QTAIM Topology Is Sensitive to Relativistic Corrections. *Chemistry Eur. J.* **2019**, *25*, 2538–2544.
- (36) Olejniczak, M.; Severo Pereira Gomes, A.; Tierny, J. A Topological Data Analysis perspective on noncovalent interactions in relativistic calculations. *Int. J. Quantum Chem.* **2020**, *120*, e26133.
- (37) Sarr, S.; Graton, J.; Montavon, G.; Pilmé, J.; Galland, N. On the Interplay between Charge-Shift Bonding and Halogen Bonding. *ChemPhysChem* **2020**, *21*, 240–250.
- (38) Guo, N.; Maurice, R.; Teze, D.; Graton, J.; Champion, J.; Montavon, G.; Galland, N. Experimental and computational evidence of halogen bonds involving astatine. *Nature Chem.* **2018**, *10*, 428–434.
- (39) Hogan, S. W.; Van Mourik, T. Competition between hydrogen and halogen bonding in halogenated 1-methyluracil: Water systems. *J. Comput. Chem.* **2016**, *37*, 763–770.
- (40) Hill, J. G.; Hu, X. Theoretical insights into the nature of halogen bonding in prereactive complexes. *Chem. Eur. J.* **2013**, *19*, 3620–3628.
- (41) Alkorta, I.; Elguero, J.; Yáñez, M.; Mó, O.; Montero-Campillo, M. M. Relativistic Effects on NMR Parameters of Halogen-Bonded Complexes. *Molecules* **2019**, *24*, 4399.
- (42) Lenthe, E. v.; Baerends, E.-J.; Snijders, J. G. Relativistic regular two-component Hamiltonians. *J. Chem. Phys.* **1993**, *99*, 4597–4610.
- (43) Řezáč, J.; Riley, K. E.; Hobza, P. Benchmark calculations of noncovalent interactions of halogenated molecules. *J. Chem. Theory Comput.* **2012**, *8*, 4285–4292.
- (44) Boys, S. F.; Bernardi, F. The calculation of small molecular interactions by the differences of separate total energies. Some procedures with reduced errors. *Mol. Phys.* **1970**, *19*, 553–566.

- (45) Pritchard, B. P.; Altarawy, D.; Didier, B.; Gibson, T. D.; Windus, T. L. New basis set exchange: An open, up-to-date resource for the molecular sciences community. *J. Chem. Inf. Model.* **2019**, *59*, 4814–4820.
- (46) Schuchardt, K. L.; Didier, B. T.; Elsethagen, T.; Sun, L.; Gurumoorthi, V.; Chase, J.; Li, J.; Windus, T. L. Basis set exchange: A community database for computational Sciences. *J. Chem. Inf. Model.* **2007**, *47*, 1045–1052.
- (47) Camiletti, G. G.; Machado, S. F.; Jorge, F. E. Gaussian basis set of double zeta quality for atoms K through Kr: Application in DFT calculations of molecular properties. *J. Comput. Chem.* **2008**, *29*, 2434–2444.
- (48) Barros, C.; de Oliveira, P.; Jorge, F.; Neto, A. C.; Campos, M. Gaussian basis set of double zeta quality for atoms Rb through Xe: application in non-relativistic and relativistic calculations of atomic and molecular properties. *Mol. Phys.* **2010**, *108*, 1965–1972.
- (49) Neto, A. C.; Muniz, E.; Centoducatte, R.; Jorge, F. Gaussian basis sets for correlated wave functions. Hydrogen, helium, first- and second-row atoms. *J. Mol. Struct. THEOCHEM* **2005**, *718*, 219–224.
- (50) Camiletti, G. G.; Neto, A. C.; Jorge, F. E.; Machado, S. F. Augmented Gaussian basis sets of double and triple zeta valence qualities for the atoms K and Sc-Kr: Applications in HF, MP2, and DFT calculations of molecular electric properties. *J. Mol. Struct. THEOCHEM* **2009**, *910*, 122–125.
- (51) de Oliveira, P. J. P.; Barros, C. L.; Jorge, F. E.; Neto, A. C.; Campos, M. Augmented Gaussian basis set of double zeta valence quality for the atoms Rb and Y-Xe: Application in DFT calculations of molecular electric properties. *J. Mol. Struct. THEOCHEM* **2010**, *948*, 43–46.
- (52) Martins, L. S. C.; de Souza, F. A. L.; Ceolin, G. A.; Jorge, F. E.; de Berrdo, R. C.; Campos, C. T. Augmented Gaussian basis sets for the elements K, Sc-Kr, Rb, and Y-Xe: Application in HF, MP2, and DFT calculations of molecular electric properties. *Comput. Theor. Chem.* **2013**, *1013*, 62–69.
- (53) Jorge, F. E.; Neto, A. C.; Camiletti, G. G.; Machado, S. F. Contracted Gaussian basis sets for Douglas-Kroll-Hess calculations: Estimating scalar relativistic effects of some atomic and molecular properties. *J. Chem. Phys.* **2009**, *130*, 064108.
- (54) Wilson, A. K.; Woon, D. E.; Peterson, K. A.; Jr., T. H. D. Gaussian basis sets for use in correlated molecular calculations. IX. The atoms gallium through krypton. *J. Chem. Phys.* **1999**, *110*, 7667–7676.
- (55) de Jong, W. A.; Harrison, R. J.; Dixon, D. A. Parallel Douglas-Kroll energy and gradients in NWChem: Estimating scalar relativistic effects using Douglas-Kroll contracted basis sets. *J. Chem. Phys.* **2001**, *114*, 48–53.
- (56) Peterson, K. A. Systematically convergent basis sets with relativistic pseudopotentials. I. Correlation consistent basis sets for the post-d group 1315 elements. *J. Chem. Phys.* **2003**, *119*, 11099–11112.

- (57) Roos, B. O.; Lindh, R.; Malmqvist, P.-A.; Veryazov, V.; Widmark, P.-O. Main group atoms and dimers studied with a new relativistic ANO basis set. *J. Phys. Chem. A* **2004**, *108*, 2851–2858.
- (58) Jurečka, P.; Hobza, P. On the convergence of the (Δ ECCSD(T)– Δ EMP2) term for complexes with multiple H-bonds. *Chem. Phys. Lett.* **2002**, *365*, 89–94.
- (59) Halkier, A.; Helgaker, T.; Jørgensen, P.; Klopper, W.; Koch, H.; Olsen, J.; Wilson, A. K. Basis-set convergence in correlated calculations on Ne, N₂, and H₂O. *Chem. Phys. Lett.* **1998**, *286*, 243–252.
- (60) Valiev, M.; Bylaska, E.; Govind, N.; Kowalski, K.; Straatsma, T.; Dam, H. V.; Wang, D.; Nieplocha, J.; Apra, E.; Windus, T.; de Jong, W. NWChem: A comprehensive and scalable open-source solution for large scale molecular simulations. *Comput. Phys. Commun.* **2010**, *181*, 1477–1489.
- (61) Nakajima, T.; Hirao, K. The higher-order Douglas-Kroll transformation. *J. Chem. Phys.* **2000**, *113*, 7786–7789.
- (62) Tierny, J.; Favelier, G.; Levine, J. A.; Gueunet, C.; Michaux, M. The topology toolkit. *IEEE Trans. Vis. Comput. Graph.* **2017**, *24*, 832–842.
- (63) Ahrens, J.; Geveci, B.; Law, C. Paraview: An end-user tool for large data visualization. *The visualization handbook* **2005**, 717.
- (64) Bader, R. F. Atoms in molecules. *Acc. Chem. Res.* **1985**, *18*, 9–15.
- (65) Bader, R. F. W.; Carroll, M. T.; Cheeseman, J. R.; Chang, C. Properties of atoms in molecules: atomic volumes. *J. Am. Chem. Soc.* **1987**, *109*, 7968–7979.
- (66) Sedlak, R.; Kolář, M. H.; Hobza, P. Polar flattening and the strength of halogen bonding. *J. Chem. Theory Comput.* **2015**, *11*, 4727–4732.
- (67) Van Der Walt, S.; Colbert, S. C.; Varoquaux, G. The NumPy array: a structure for efficient numerical computation. *Comput. Sci. Eng.* **2011**, *13*, 22–30.
- (68) Hunter, J. D. Matplotlib: a 2D graphics environment. *Comput. Sci. Eng.* **2007**, *9*, 90–95.
- (69) Riley, K. E.; Tran, K.-A.; Lane, P.; Murray, J. S.; Politzer, P. Comparative analysis of electrostatic potential maxima and minima on molecular surfaces, as determined by three methods and a variety of basis sets. *J. Comput. Sci.* **2016**, *17*, 273–284.
- (70) Grabowski, S. J. Hydrogen bonding strength measures based on geometric and topological parameters. *J. Phys. Org. Chem.* **2004**, *17*, 18–31.
- (71) Bankiewicz, B.; Matczak, P.; Palusiak, M. Electron density characteristics in bond critical point (QTAIM) versus interaction energy components (SAPT): the case of charge-assisted hydrogen bonding. *J. Phys. Chem. A* **2012**, *116*, 452–459.

- (72) Franconetti, A.; Frontera, A. Like-like tetrel bonding interactions between Sn centres: a combined ab initio and CSD study. *Dalton Trans.* **2019**, *48*, 11208–11216.
- (73) Amezaga, N. J. M.; Pamies, S. C.; Peruchena, N. M.; Sosa, G. L. Halogen bonding: a study based on the electronic charge density. *J. Phys. Chem. A* **2010**, *114*, 552–562.
- (74) Bauzá, A.; Quiñonero, D.; Frontera, A.; Deyà, P. M. Substituent effects in halogen bonding complexes between aromatic donors and acceptors: a comprehensive ab initio study. *Phys. Chem. Chem. Phys.* **2011**, *13*, 20371–20379.

Supplementary Information

From the main text of the article we repeat that the energies of complexes and their interacting subsystems were calculated using the CCSD(T) method, wherever it was computationally feasible. The calculations in AQZP and aug-cc-pVQZ basis set of all complexes except for the smallest one – $\text{F}_3\text{CBr}\cdots\text{OCH}_2$, could only be carried out at the MP2, and the well-established focal-point scheme was applied to obtain an estimate of the $E_Q(\text{CCSD(T)})$ energies.

$$E_X(\text{CCSD(T)}) = E_X(\text{MP2}) + \Delta E_{X-1}(\text{CCSD(T)}) \quad (\text{S1})$$

where $\Delta E_{X-1}(\text{CCSD(T)})$ is the difference of CCSD(T) and MP2 energies in basis set with lower cardinality “X – 1”.

Table S1: Number of eliminated basis functions due to linear dependence / total number of AO basis functions for complexes containing iodine.

Complex	Basis set	X=D	X=T	X=Q
$\text{F}_3\text{CI}\cdots\text{OCH}_2$	AXZP			
	ANO-RCC-X			
	cc-pVXZ-PP			
	aug-cc-pVXZ-PP			
$\text{PheI}\cdots\text{SHCH}_3$	AXZP	2/346	10/687	203 ⁽¹⁾ /1216
	ANO-RCC-X	-	-	2/742
	cc-pVXZ-PP	-	-	1/781
	aug-cc-pVXZ-PP	3/301	12/634	24/1150
$\text{F}_3\text{CI}\cdots\text{C}_6\text{H}_6$	AXZP	2/358	11/703	33 ⁽²⁾ /1231
	ANO-RCC-X	-	-	3/740
	cc-pVXZ-PP	-	-	1/797
	aug-cc-pVXZ-PP	3/316	11/653	23/1168

linear dependence threshold [a.u.]: ⁽¹⁾ $7,5\cdot 10^{-3}$; ⁽²⁾ $3,0\cdot 10^{-5}$

Table S2: CCSD(T) interaction energies [kcal/mol] of complexes containing bromine. Interaction energies in parentheses are obtained using focal-point approximation according to Eq. S1.

Complex	Basis set	CBS	X=D	X=T	X=Q
F ₃ CBr···OCH ₂	XZP	-2.65 (-2.78)	-0.63	-1.35	-2.10
	cc-pVXZ	-2.92 (-2.79)	-1.14	-1.92	-2.50
	AXZP	-3.04 (-2.98)	-2.21	-2.57	-2.81
	aug-cc-pVXZ	-3.00 (-2.99)	-2.37	-2.69	-2.87
	XZP-DKH	-2.79 (-2.92)	-0.77	-1.52	-2.26
	cc-pVXZ-DKH	-3.06 (-2.93)	-1.30	-2.07	-2.64
	aug-cc-pVXZ-DKH	-3.13 (-3.13)	-2.53	-2.83	-3.01
	ANO-RCC-X	-3.14 (-3.15)	-1.80	-2.54	-2.89
	cc-pVXZ-PP	-3.10 (-2.97)	-1.36	-2.10	-2.68
	aug-cc-pVXZ-PP	-3.17 (-3.17)	-2.54	-2.86	-3.04
PheBr···SHCH ₃	XZP	-1.94	-0.05	-0.63	-1.39
	cc-pVXZ	-2.24	-0.46	-1.22	-1.81
	AXZP	-2.22	-1.38	-1.87 ^(a)	-2.07 ^(a)
	XZP-DKH	-2.06	-0.02	-0.77	-1.51
	aug-cc-pVXZ	-2.25	-1.59	-1.98 ^(a)	-2.13 ^(a)
	cc-pVXZ-DKH	-2.35	-0.60	-1.34	-1.92
	aug-cc-pVXZ-DKH	-2.36	-1.72	-2.09 ^(a)	-2.25 ^(a)
	ANO-RCC-X	-2.41	-0.72	-1.79	-2.15
	cc-pVXZ-PP	-2.38	-0.62	-1.37	-1.95
	aug-cc-pVXZ-PP	-2.39	-1.73	-2.13 ^(a)	-2.28 ^(a)
F ₃ CBr···C ₆ H ₆	XZP	-2.84	-0.01	-1.10	-2.10
	cc-pVXZ	-3.03	-0.83	-1.96	-2.58
	AXZP	-2.99	-2.13	-2.76 ^(a)	-2.89 ^(a)
	aug-cc-pVXZ	-3.02	-2.34	-2.80 ^(a)	-2.93 ^(a)
	XZP-DKH	-2.96	-0.08	-1.20	-2.22
	cc-pVXZ-DKH	-3.11	-0.94	-2.06	-2.67
	aug-cc-pVXZ-DKH	-3.19	-2.43	-2.89 ^(a)	-3.06 ^(a)
	ANO-RCC-X	-3.13	-1.59	-2.55	-2.88
	cc-pVXZ-PP	-3.13	-0.94	-2.09	-2.69
	aug-cc-pVXZ-PP	-3.13	-2.44	-2.91 ^(a)	-3.04 ^(a)

^(a) Energy calculated according to Eq. S1.

Table S3: CCSD(T) interaction energies [kcal/mol] of complexes containing iodine.

Complex	Basis set	CBS	X=D	X=T	X=Q
F ₃ CI···OCH ₂	XZP	-2.86	-0.98	-2.08	-2.54
	AXZP	-4.09	-2.41	-2.93	-3.60
	ANO-RCC-X	-4.19	-2.20	-3.00	-3.69
	XZP-DKH	-3.42	-1.34	-2.38	-2.98
	cc-pVXZ-PP	-4.09	-1.97	-2.85	-3.57
	aug-cc-pVXZ-PP	-4.19	-3.33	-3.75	-4.00
PheI···SHCH ₃	XZP	-1.99	-0.89	-1.16	-1.64
	AXZP	-2.75	-1.54	-2.22 ^(a)	-2.53 ^(a)
	ANO-RCC-X	-3.27	-0.66	-1.97	-2.72
	XZP-DKH	-2.58	-0.41	-1.48	-2.11
	cc-pVXZ-PP	-3.19	-0.97	-1.91	-2.65
	aug-cc-pVXZ-PP	-3.20	-2.27	-2.82 ^(a)	-3.04 ^(a)
F ₃ CI···C ₆ H ₆	XZP	-2.85	-0.24	-2.02	-2.50
	AXZP	-3.65	-2.54	-3.44 ^(a)	-3.56 ^(a)
	ANO-RCC-X	-4.14	-1.58	-2.82	-3.58
	XZP-DKH	-3.15	-0.55	-2.25	-2.77
	cc-pVXZ-PP	-3.98	-1.31	-2.72	-3.45
	aug-cc-pVXZ-PP	-4.00	-3.02	-3.71 ^(a)	-3.88 ^(a)

^(a) Energy calculated according to Eq. S1